

Highly Sensitive Biosensing with Solid-State Nanopores Displaying Enzymatically Reconfigurable Rectification Properties

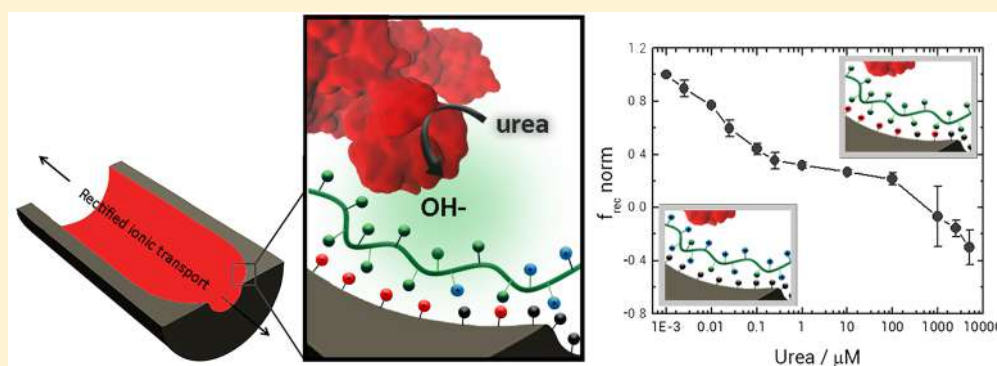
Gonzalo Pérez-Mitta,^{*,†,||,⊥} Ana S. Peinetti,^{†,||,#} M. Lorena Cortez,[†] María Eugenia Toimil-Molares,[‡] Christina Trautmann,^{‡,§} and Omar Azzaroni^{*,†,||}

[†]Instituto de Investigaciones Físicoquímicas Teóricas y Aplicadas (INIFTA), Departamento de Química, Facultad de Ciencias Exactas, Universidad Nacional de La Plata (UNLP), CONICET, Boulevard 113 y 64, 1900 La Plata, Argentina

[‡]GSI Helmholtzzentrum für Schwerionenforschung, 64291 Darmstadt, Germany

[§]Technische Universität Darmstadt, 64287 Darmstadt, Germany

S Supporting Information



ABSTRACT: Molecular design of biosensors based on enzymatic processes taking place in nanofluidic elements is receiving increasing attention by the scientific community. In this work, we describe the construction of novel ultrasensitive enzymatic nanopore biosensors employing “reactive signal amplifiers” as key elements coupled to the transduction mechanism. The proposed framework offers innovative design concepts not only to amplify the detected ionic signal and develop ultrasensitive nanopore-based sensors but also to construct nanofluidic diodes displaying specific chemo-reversible rectification properties. The integrated approach is demonstrated by electrostatically assembling poly(allylamine) on the anionic pore walls followed by the assembly of urease. We show that the cationic weak polyelectrolyte acts as a “reactive signal amplifier” in the presence of local pH changes induced by the enzymatic reaction. These bioinduced variations in proton concentration ultimately alter the protonation degree of the polyamine resulting in amplifiable, controlled, and reproducible changes in the surface charge of the pore walls, and consequently on the generated ionic signals. The “iontronic” response of the as-obtained devices is fully reversible, and nanopores are reused and assayed with different urea concentrations, thus ensuring reliable design. The limit of detection (LOD) was 1 nM. To the best of our knowledge, this value is the lowest LOD reported to date for enzymatic urea detection. In this context, we envision that this approach based on the use of “reactive signal amplifiers” into solid-state nanochannels will provide new alternatives for the molecular design of highly sensitive nanopore biosensors as well as (bio)chemically addressable nanofluidic elements.

KEYWORDS: Solid-state nanopores, nanofluidic devices, nanochannels, biosensing, urea sensing

In recent years, nanofluidic devices such as nanopores and nanochannels have attracted much attention due to the development of promising technological applications in diverse fields such as sensing, nanofluidic actuation and delivery, water desalination and energy conversion, among others.^{1–5} However, the field of nanofluidics itself is only starting to show its potential, and a prominent role in future technologies is expected.⁶ Nanofluidics deals with the transport of ionic and molecular species upon the application of force fields both electrical and mechanic in highly confined environments, typically in the femtoliter regime.⁷ Early results showed that rare phenomena, such as unipolar conductivity, ionic rectification, or molecular

sieving by size and charge, arise from this confinement.^{8,9} The explanation and manipulation of such phenomena (previously observed only in biological systems) are currently the aim of many research projects in different fields, especially toward biosensing and micrototal-analysis systems (μ TAS) applications.

Some specific features observed in nanofluidic devices which are related to their exquisite control over ionic transport have been termed “iontronics” due to their resemblance with features

Received: March 29, 2018

Revised: April 25, 2018

Published: April 26, 2018

observed in electronic components.¹⁰ The idea behind this relatively new field is the realization of fluidic components that would allow designing actual molecular circuits. To date, different nanofluidic components such as ionic rectifiers, diodes, or transistors have been achieved by combining nanofabrication with surface modification techniques, showing that it is possible to selectively control in an accurate manner the transport of different ionic species by applying experimentally controlled stimuli.^{11,12} These concepts are heavily inspired by biological systems performing different functions like transfer of information, building up gradients of energy, or performing complex biochemical reactions that depend on the precise control of the amounts of specific molecules. The process is typically based on selectively transporting ions and molecules through high-impedance membranes ($10^{16} \Omega$).^{13–15}

Moreover, just like in biological systems, abiotic nanofluidic devices have the potential to allow not only the separation and distribution of different charged species but also its determination by transducing the presence of a certain molecule into a readable output.¹⁶ In this regard, two general approaches have been used for nanofluidic sensing. The most commonly used is based on the Coulter counter principle of resistive-pulse sensing (RPS), and it determines the size of a molecule by observing the change in the current when the molecule passes through and thus blocks the pore.¹⁷ This is a time-resolved type of measurement that needs equipment with good frequency resolution. Specific statistical analysis is required, and because of the fact that it depends on the steric blockage of the fluidic channel, the size of molecules that can be sensed is limited. The other, perhaps less explored procedure, consists of steady-state measurements performed by sweeping the transmembrane potential at low enough frequencies (<0.1 Hz) and measuring the complete current–voltage characteristics.^{18,19} In this kind of experiment, a broader picture of the behavior of a particular nanofluidic device can be obtained. For example, for the case of nanofluidic diodes, systems that rectify the ionic current at opposite polarities, current/voltage characteristics show a nonlinear tendency that can be ultimately related with the geometry and charge of the ionic diode (nanochannel). As demonstrated, asymmetric geometries or charge distributions lead to current rectification.²⁰ This implies that modifying the magnitude or sign of the surface charge of the nanochannel concomitantly changes the magnitude or direction of the rectified current, because of the inversion of the electric potential distribution across the nanochannels.²¹ Because of this, it is possible to sense molecules that produce small changes in the surface charge of these ionic diodes with potentially high sensitivity.²² In this sense, we could think of ionic diodes (asymmetric nanochannels) as amplifiers that—resulting from confinement effects—enhance the response to small chemical conversions that otherwise would be impossible to sense using bulk or common surface methods. This concept is often referred to as “iontronic amplification”, which is in a way a concept related to surface-enhanced Raman spectroscopy (SERS) for which nanometric confinement of electronic surface modes enhance the signal produced by specific molecules in solution.²³ In this regard, biosensing with nanofluidic diodes is foreseen as one of the major applications of these interesting nanosystems. To this end, early attempts have previously explored different strategies, such as direct attaching of responsive molecules to the surface of the pores.^{24–27} In particular, the integration of enzymatic processes into solid-state nanopores confer them outstanding specificity on target analytes resulting from biological recognition.

Manipulating the specificity and selectivity of solid-state nanopores with enzymatic architectures available to catalyze specific biochemical reactions has attracted considerable attention during recent years. Fink and workers²⁸ first proposed the fabrication of urea sensors by attaching urease to the inner walls of etched ion tracks within thin polymer foils, i.e., polymer nanochannels. They demonstrated that the presence of urea affects the resistance and capacitance of the nanosystem. Then, Jiang and co-workers²⁹ described the conjugation of glucose oxidase into conical nanopores to detect glucose via changes in the transmembrane ionic current arising from changes in the protonation of the enzyme residues due to local pH changes induced by the enzymatic reaction. However, relying on the protonation of enzyme residues can pose limitations to the transduction mechanism because of the limited number of protonable groups on the enzyme. In addition, the use of covalent immobilization strategies might affect the enzymatic activity and reduce the number of protonable groups. On the other hand, one may also consider designing nanofluidic elements that can switch their rectification direction in the presence of specific chemical species of biological interest, such as, for example, a nanofluidic diode that can reverse the passage of anions and cations in the presence of a specific analyte. The achievement of such a system would pave the way toward the creation of chemically reconfigurable nanofluidic circuits. Interestingly, Matile and his collaborators³⁰ proposed the use of “reactive amplifiers” to covalently capture elusive analytes after enzymatic signal generation and drag them into synthetic pores for blockage. This notion offers us a particularly suitable framework for exploration, provided that the use of interfacial architectures that could alter the magnitude and sign of the nanopore surface charge after the enzymatic recognition might confer not only amplified sensing capabilities to the nanopores but also reversible rectification properties. Taking into account these concepts and being aware of the promising features of enzymatic biosensing in nanopores, we have taken this new paradigm a step further and propose a new approach to design nanofluidic biosensors based on the iontronic amplification of an enzymatic reaction by electrostatically incorporating polyelectrolytes into the nanopore as “reactive signal amplifiers”. As an example, we demonstrated the versatility of the proposed strategy by electrostatically assembling poly(allylamine) (PAH) (a cationic weak polyelectrolyte) on the anionic surface of asymmetrically shaped nanochannels and subsequently assembling urease on the PAH layer. In the presence of urea, urease degrades the analyte into ammonia and carbon dioxide leading to a change in the protonation degree of the polyamine and ultimately changing the charge state of the surface of the solid-state nanochannel. This procedure is shown to be both reversible and reproducible while yielding a limit of detection (LOD) of 1 nM which to the best of our knowledge is the lowest value reported to date for urea with a reaction time of <1 min. Additionally, we show that the rich interplay between the native anionic charges of the nanopores and the cationic poly(allylamine)—which leads to a zwitterionic pore wall—can be modulated by the enzymatic process in such a way that the urea-responsive nanofluidic device displays fully tunable and reversible ionic rectification. We expect that this work has profound implications not only for the supramolecular design of ultrasensitive nanopore biosensors but also for design and development of reconfigurable nanofluidic circuits driven by specific chemical inputs.

The success of the PAH modification procedure was verified by I – V measurements testing if the net charge of the nanochannel

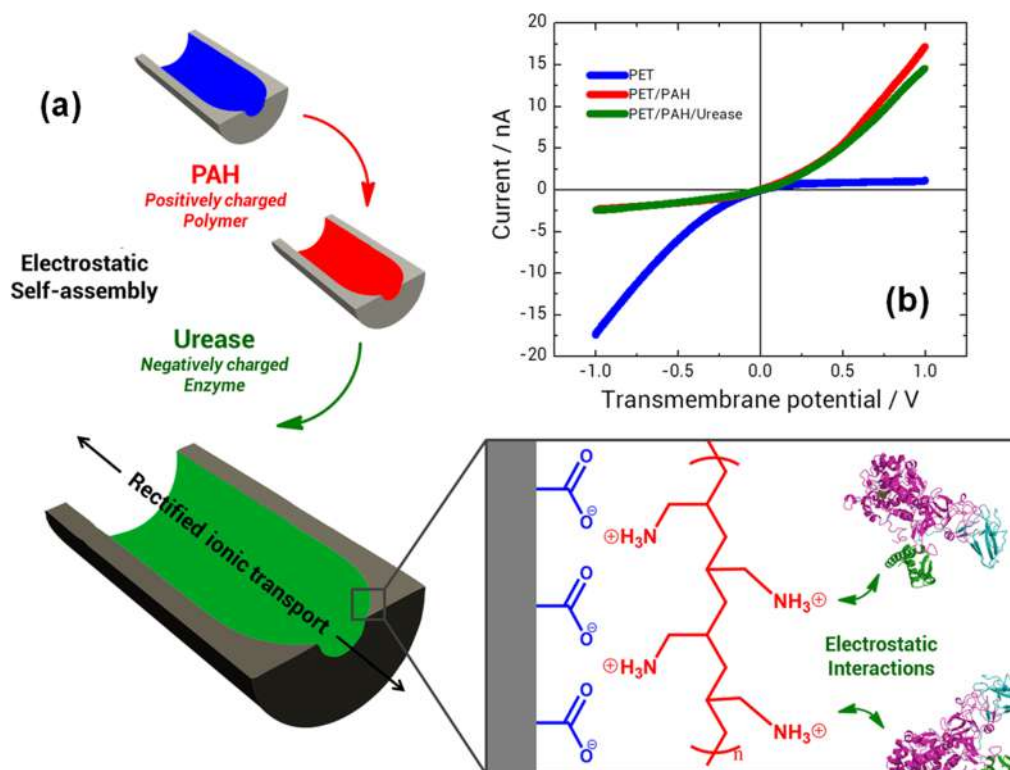


Figure 1. (a) Scheme depicting the fabrication procedure of the urease-poly(allyl amine)-nanochannel and the electrostatic interactions taking place on the nanochannel surface. (b) Current–voltage curves measured before and after each modification step at pH 6, bare nanochannel (blue curve), after the modification with PAH (red curve) and after subsequent modification with urease (green curve).

changed from negative (carboxylate groups) to positive (amine groups) at the working solution pH (~ 5.5). Changing the surface charge of the nanochannels produces a switch in its ionic selectivity, which can be observed as a change in the direction of the rectified ionic currents (or by a change in the rectification efficiency) at opposite polarities. This current gating process is illustrated in Figure 1.

The PAH modification procedure is very robust^{31,32} and has the great advantage that it allows obtaining an “amphoteric” surface in a simple manner. This “amphoteric” surface generated by the electrostatic assembly of cationic PAH on the carboxylate-bearing wall of the poly(ethylene terephthalate) (PET) nanopores (Figure 1) represents a useful resource in nanofluidics to control the ion selectivity of nanofluidic devices by controlling the proton concentration in solution. Therefore, the PAH-modified PET nanochannel (PET/PAH) shows a pH-dependent behavior that allows reaching different rectification efficiencies at different pH values and even changing the direction of the rectification. This pH-dependent behavior was characterized by measuring the current–voltage characteristics, while changing the solution pH by adding dropwise HCl or NaOH solutions to explore the complete functional pH range. The nanofluidic titration curve is presented in Figure S2. As expected, these results show an isoelectric region at pH values close to 7.³¹

Once the surface of the nanochannels was modified with PAH, the urease (Ur) was electrostatically incorporated into the nanopore at pH 7.4 (HEPES buffer). Under these conditions the enzyme is negatively charged since it has an isoelectric point of 5.2.³³ The modification procedure was also confirmed by measuring I – V curves (Figure 1). In this case, the change in ionic currents and rectification efficiency did not show a reversion of the rectification efficiency direction as with the PAH

modification, mainly because the amount of electrostatic charges exposed by the enzyme is not high enough to overcompensate the charges stemming from the PAH layer. However, the I – V curves showed a slight decrease in the rectified current, which might be related to the reduction of the nanochannel cross-section due to the presence of the enzyme.

After the incorporation of urease, current–voltage characteristics were measured again at different pHs. The shape of the rectification efficiency versus pH curve was qualitatively the same as with PAH only (Figure 2) but showing systematically lower rectification efficiencies for each pH. This is understandable since a certain fraction of the positive charges of the PAH layer are neutralized by the protein, therefore reducing the number of available charges contributing to the net charge of the nanochannel. It is important to note that even though the presence of the protein on the surface of the PAH-modified nanochannels (PET/PAH) reduces the magnitude of ionic currents through the pore, it does not preclude the pH responsiveness of the nanochannel maintaining its amphoteric behavior.

Figure 2 shows the response of a urease-PAH-modified nanochannel (PET/PAH/Ur) as a function of pH. Changing the pH from acidic to basic conditions leads to the reversion of the rectification direction, and consequently to the reversion in the selectivity of the channel. To use this device as an iontronic amplifier, it was important to determine the pH value at which the sensing response is enhanced to a greater extent, i.e., a region where the gating of the ionic currents is greater. By inspection of Figure 2, this region was found to lie within the range of pH between 6 and 7.

The next feature to take into account is the activity of the enzyme which is known to peak around pH 7.4 decreasing toward more acidic or basic conditions.³⁴ As shown in the reaction below,

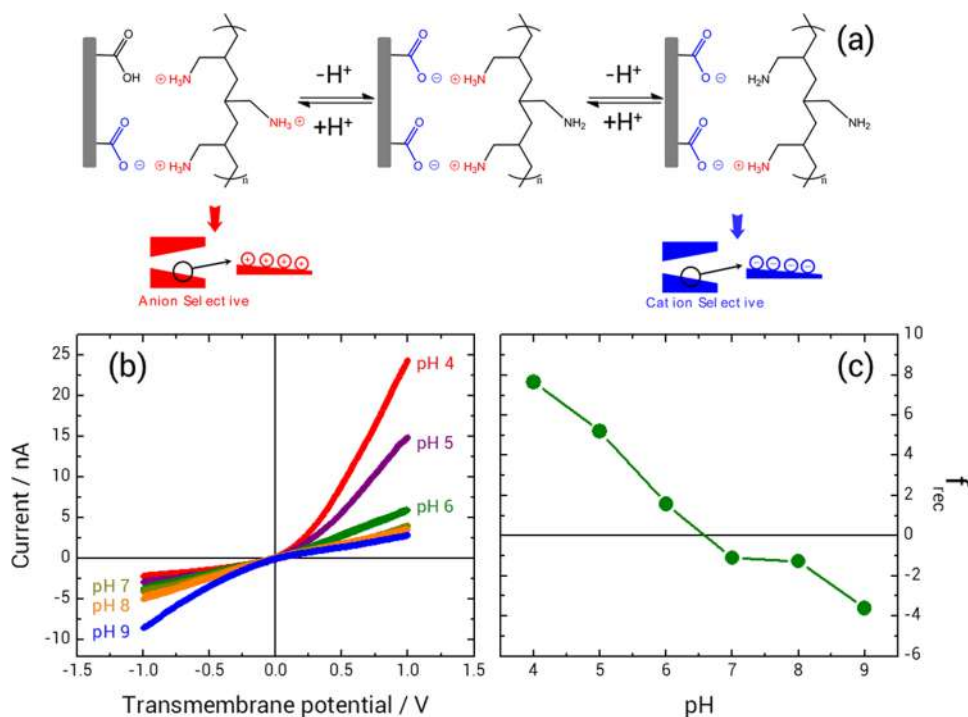
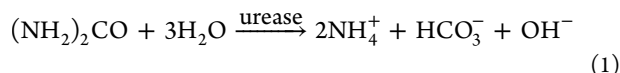


Figure 2. (a) Schemes depicting the different protonation states of the amphoteric nanochannel and the resulting charge and selectivity. The urease is not included in the schemes for the sake of simplicity. (b) I - V curves and (c) rectification efficiency versus pH after the modification of the PAH-coated nanochannel with urease (PET/PAH/U). Curves were measured in 0.1 M KCl with dropwise addition of NaOH or HCl to reach each pH value.

urease catalyzes the decomposition of urea into ammonium and carbonic acid³⁵



During the course of the reaction, the pH of the solution is increased locally; actually it was recently shown that the pH can be shifted several units in a urea-concentration dependent fashion reaching pH as high as 9.³⁶ However, being able to observe such pH changes requires a large amount of proteins anchored to the surface because a detectable pH shift requires the reaction of a large amount of urea. On the other hand, the same extent of products generated inside a nanochannel would produce a higher change in the local pH due to the confinement into a femtoliter volume, and therefore, by increasing the concentration of urea it would be possible to move across the nanofluidic titration curve from left to right (Figure 2). This could be accomplished by indirect generation of hydroxyl ions that, in turn, shift the protonation degree of the PAH monomeric units toward the deprotonated state. By adding different concentrations of urea to solutions with different pH values, we found that pH 5 prompts the best iontronic amplification. We hypothesize that at this pH the relation between the regions on the titration curve that yields the maximum amplification of the enzymatic reaction and the region of highest enzymatic activity is maximal.

Once the working pH was set at 5, the urea-dependent behavior of the PET/PAH/Ur nanochannel was tested by using aqueous urea solutions with concentrations ranging from 1 nM to 5 mM. Upon increasing the amount of urea in solution, the nanofluidic system shifted progressively from anion selectivity to cation selectivity, or in rectification terms, from positive rectification to negative rectification. Figure 3 shows the normalized rectification efficiency versus the concentration of urea in

solution. The trend is similar to the one observed for the titration curve. This is not surprising because of the fact that the increasing amount of urea is expected to shift the protonation degree of the PAH to lower values through its degradation by the urease. At low urea concentrations the rectification efficiency (f_{rec}) is positive, which according to our convention means that the surface of the nanochannel is positively charged, and the permselectivity of the channels concerns anions. Upon an increase in the concentration, the rectification efficiency linearly decreased, up to a concentration of 1 μM . This decrease is attributed to the deprotonation of both primary amines of the PAH and carboxylate groups of the surface of the unmodified nanochannels. Higher concentrations, up to 100 μM , did not produce a significant change of the rectification efficiency. Within this region, both the PAH and the carboxylate groups are significantly charged, possibly producing an electrically neutral surface. According to previous reports, this electrostatically neutral region is termed the isoelectric region.³¹ Further increase of the concentration (>100 μM) induced the increment of the rectification efficiency in the negative direction. According to our convention, this means an increase in the negative surface charge of the nanochannel and a permselectivity toward cations. The increment of the negative charge saturated at a concentration of 5 mM.

For verification of the reproducibility of the fabrication procedure and functional response of the system, these experiments were repeated using different single nanochannels. From sample to sample, the nanochannel signal slightly differs because of small differences in the foil, etching procedure, and thus resulting pore size. For comparison of different samples, the rectification efficiencies (f_{rec}) were normalized by dividing each value with the maximum absolute value obtained for a given nanochannel (see eq S2 in the SI file). A remarkable reproducibility was found between different experiments by comparing normalized

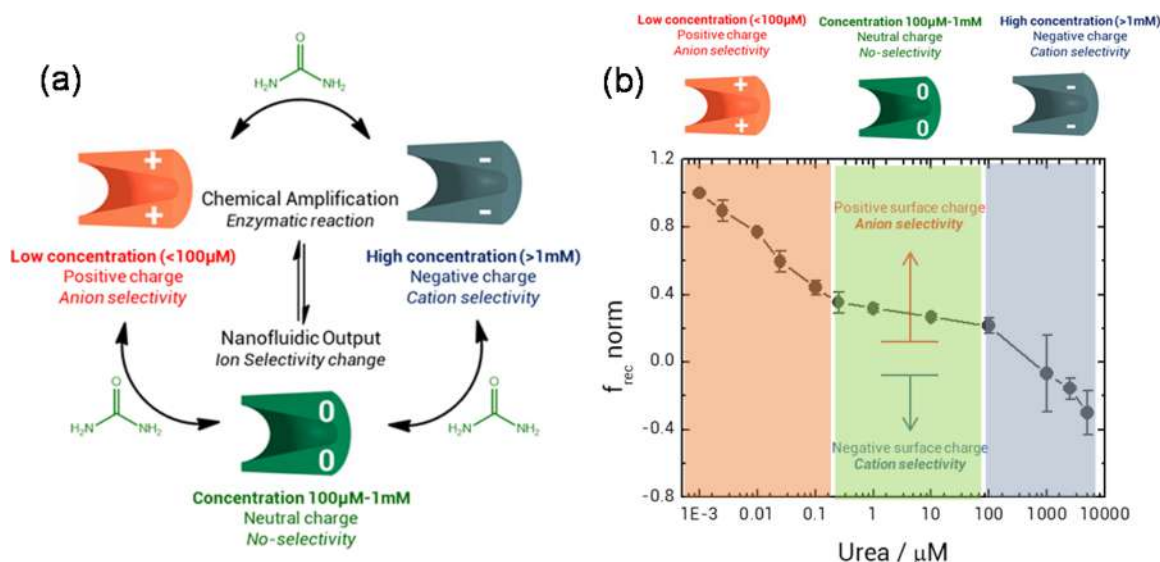


Figure 3. (a) Scheme depicting the relation between the biochemical degradation of urea and the nanofluidic output of the nanochannel through the amplification of the enzymatic reaction. Low concentration leads to positively charged surfaces while high concentration leads to negatively charged surfaces with concomitant changes in the ionic selectivity of the nanochannels. (b) Normalized rectification efficiencies ($f_{\text{rec-norm}}$) and error bars were obtained from the results for three different nanochannels. The solid line has been introduced to guide the eye.

rectification efficiencies ($f_{\text{rec-norm}}$; Figure 3; see Figure S4 in the SI file for further details).

Our data provide clear evidence that regulating the concentration of urea in solution allows a wide variety of nanofluidic operations including permselective current gating and selectivity switching. This type of chemically reconfigurable system is of great interest in nanofluidics if we consider that a specific preset chemical input can finely regulate the direction and the magnitude of the ion flux through the nanochannels. Concerning this matter, it is important to assess the kinetic response in the presence of the chemical stimulus, i.e., how fast the system responds to the presence of urea in solution. We thus performed a time-resolved measurement by determining the transmembrane current of a PET/PAH/Ur nanochannel while applying a constant voltage of 1 V (Figure 4). After several minutes of

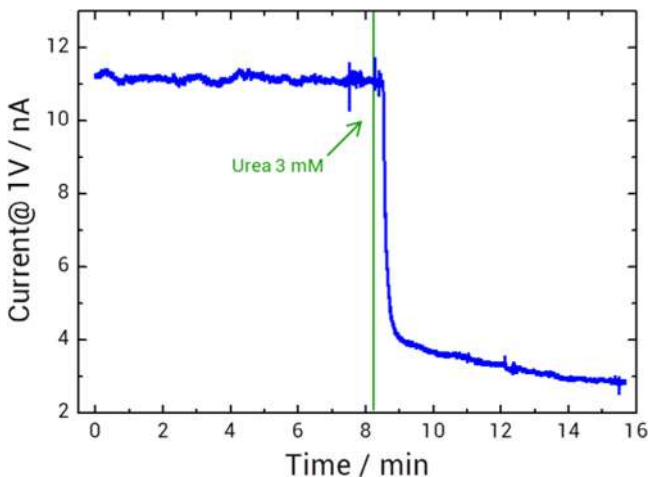


Figure 4. Kinetic response of a PET/PAH/Ur nanochannel to the addition of urea up to a concentration of 3 mM in solution while measuring the transmembrane current at 1 V.

continuous current measurements, a small amount of urea (0.18 mg) was added to the solution in the conductivity cell up to

a final concentration of 3 mM. The response was almost immediate; within a few seconds the current steeply decreased indicating that the enzymatic degradation of urea generates an immediate reduction of the protonation degree of the PAH and a concurrent decrease in the anion-driven current.

Up to now, we have discussed the general response of the system to urea in solution as a chemical gate for the ionic permselective transport providing a promising system for nanofluidic biosensing applications. Figure 3 illustrates that urea concentration can be analyzed in a broad range and shows a linear relationship for urea concentrations between 1 nM and 1 μM , where the amplification capability of the system is maximum. Higher concentrations already fall into the isoelectric region. The limit of detection (LOD) resulting from measurements with our biosensing nanopore was 1 nM. At this point, we should note that lower LOD values were reported for enzyme-free biosensors.^{37,38} However, it is well-known that, despite the fact that enzyme-free biosensors are very sensitive, their selectivity is very poor. On the contrary, enzyme-based sensors typically exhibit higher LOD values, but they display excellent selectivity because of the high specificity of the enzymes.³⁹ This explains why it is important to actively endeavor to devise strategies for increasing the sensitivity of enzymatic biosensors to create highly sensitive and highly specific sensing platforms. In our case, the combination of the high specificity of the enzyme (urease) with the sensitivity of the nanopore transducer boosted by the “reactive signal amplifier” led to a high-sensitivity urea sensor. To the best of our knowledge, 1 nM is the lowest LOD value reported for enzymatic urea detection⁴⁰ (for a detailed comparison of characteristics of different enzymatic urea biosensors, refer to Table S1 in the SI file). Figure 5 shows the linear region of the semilog plot of f_{rec} vs urea concentration including the error bars calculated as the standard deviation of the values measured for three different nanochannels. The behavior in this region was found to be highly reproducible. As can be seen in Figure 5, the normalized rectification efficiency ($f_{\text{rec-norm}}$) as a function of the logarithm of concentration of urea follows a linear behavior.

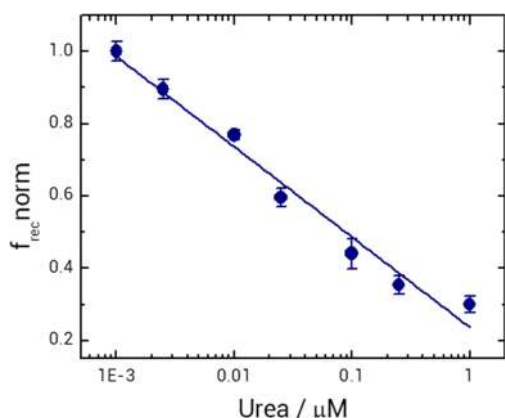


Figure 5. Normalized rectification efficiencies versus urea concentration obtained from the data of three different PET/PAH/Ur nanochannels.

In addition to reproducibility tests of the complete system, we also investigated the reversibility of the nanofluidic biosensor. In particular, we were interested in assessing whether the system was still responsive after being exposed to high concentrations of urea. To address this point, we carried out experiments by successively changing the electrolyte solution from a urea-free solution to a 1 mM urea solution, which is close to the saturation region. I – V curves were measured for each cycle, and the rectification efficiencies were calculated and plotted successively (Figure 6)

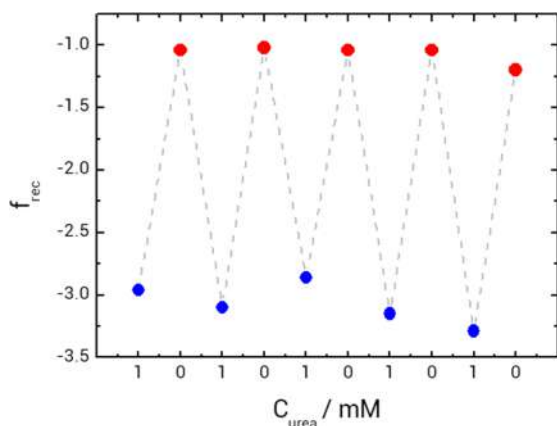


Figure 6. Reversibility tests for a PET/PAH/Ur nanochannel. The rectification efficiencies were calculated using 0.1 M KCl solutions containing either 0 (red dots) or 1 (blue dots) mM urea at pH 6.

which allows us to clearly illustrate the high reversibility of the system. After we performed 6 repetition cycles, the nanofluidic biosensor did not lose its responsive behavior, thus implying that the device could be used several times without compromising its performance.

In conclusion, nanofluidic experiments demonstrate the potency of enzymatic processes in the presence of “reactive signal amplifiers” as a key enabling approach to set, modulate, reconfigure, and amplify the biospecific responsiveness of solid-state nanopores. The conceptual framework is based on the strong dependence of the ionic transport properties of nanofluidic devices—and especially nanofluidic diodes—on the sign and magnitude of their surface charges. Combining this strong dependence with the incorporation of a weak polyelectrolyte, poly(allyl amine) (PAH), that renders the nanofluidic device an amphoteric behavior, the construction of a highly sensitive device for the detection of local pH changes can be realized. Additional

incorporation of urease into the PAH-modified nanopore via electrostatic assembly yields supramolecular integration of molecular recognition elements into the device. The transduction mechanism of the nanopore biosensor operates according to the local pH changes induced by the enzymatic decomposition of urea into ammonia and carbon dioxide. Our results demonstrate that the proposed mechanism based on “reactive signal amplifiers” allows the fine control of the nanofluidic output; i.e., ionic currents are tailored by varying the amount of urea in solution. In particular, the fast and high responsiveness of the urease-equipped amphoteric nanofluidic device to urea concentration makes it a highly sensitive enzymatic biosensor with a limit of detection of 1 nM. Furthermore, this system was proven to be highly reproducible and reversible, two fundamental features required for a technologically applicable biosensing device. Another important aspect that deserves particular attention is that this concept can be further applied to other combinations of weak polyelectrolytes and “pH-shifting” enzymes, therefore becoming a valuable strategy to design and construct nanofluidic biosensors. Additionally, this approach also offers accurate control over the reversible reconfiguration of anion-selective and cation-selective rectified transport as a function of a given chemical input. This is fundamentally interesting chemistry with strong implications for nanofluidics since these significant changes in transport properties stemming from the nanoconfined enzymatic process could be harnessed as a (bio)chemical actuation mechanism in nanofluidic circuits.

Taken all together, our set of experiments introduces a new concept to design nanopore biosensors and chemically reconfigurable nanofluidic elements based on the exquisite synergy arising from the combination of the remarkable physical characteristics of asymmetric nanopores, the chemical richness of polyelectrolyte assembly, and the unsurpassed specificity of enzymatic recognition. We envision that further extrapolation of these notions and concepts relying on the use of “reactive amplification” to other enzymatic systems will open up new opportunities to devise new, highly sensitive nanopore biosensors as well as to build up (bio)chemically addressable nanofluidic circuitry.

■ ASSOCIATED CONTENT

📄 Supporting Information

The Supporting Information is available free of charge on the ACS Publications website at DOI: 10.1021/acs.nanolett.8b01281.

Experimental details on nanochannel fabrication, modification with PAH and urease, and current–voltage measurements; definition of rectification efficiency; SEM characterization; and additional I – V measurements of functionalized nanochannels (PDF)

■ AUTHOR INFORMATION

Corresponding Authors

*E-mail: gperezmitta@inifta.unlp.edu.ar.

*E-mail: azzaroni@inifta.unlp.edu.ar. Phone: +54-221-425-7430. website: <http://softmatter.quimica.unlp.edu.ar>

ORCID

Omar Azzaroni: 0000-0002-5098-0612

Present Addresses

[†]G.P.-M.: Laboratory of Molecular Neurobiology and Biophysics, Howard Hughes Medical Institute, The Rockefeller University, 1230 York Avenue, New York, New York 10065, United States.

#A.S.P.: Department of Chemistry, University of Illinois at Urbana-Champaign, 505 South Mathews Avenue, Urbana, Illinois 61801, United States.

Author Contributions

^{||}G.P.-M. and A.S.P. contributed equally to this work and should be considered as co-first authors.

Notes

The authors declare no competing financial interest.

ACKNOWLEDGMENTS

The authors acknowledge financial support from ANPCyT (PICT 2010-2554, PICT-2013-0905, PICT-2016-1680) and from the Deutsche Forschungsgemeinschaft (DFG-FOR 1583). G.P.-M. and A.S.P. acknowledge CONICET for a doctoral and postdoctoral fellowship, respectively. M.L.C. and O.A. are staff members of CONICET. M.E.T.-M. and C.T. acknowledge support by the LOEWE project iNAPO funded by the Hessen State Ministry of Higher Education, Research and Arts.

REFERENCES

- (1) (a) Daiguji, H. *Chem. Soc. Rev.* **2010**, *39*, 901–911. (b) Xu, H.; Wei, G.; Lei, J. *Chem. Soc. Rev.* **2011**, *40*, 2385–2401. (c) Choi, Y.; Baker, L. A.; Hillebrenner, H.; Martin, C. R. *Phys. Chem. Chem. Phys.* **2006**, *8*, 4976–4988. (d) Wen, L.; Tian, Y.; Ma, J.; Zhai, J.; Jiang, L. *Phys. Chem. Chem. Phys.* **2012**, *14*, 4027–4042. (e) Shang, Y.; Zhang, Y.; Li, P.; Lai, J.; Kong, X.-Y.; Liu, W.; Xiao, K.; Xie, G.; Tian, Y.; Wen, L.; Jiang, L. *Chem. Commun.* **2015**, *51*, 5979. (f) Zhu, Y.; Zhan, K.; Hou, X. *ACS Nano* **2018**, *12*, 908–911. (g) Hou, X.; Zhang, H.; Jiang, L. *Angew. Chem., Int. Ed.* **2012**, *51*, 5296–5307.
- (2) (a) Yameen, B.; Ali, M.; Neumann, R.; Ensinger, W.; Azzaroni, O.; Knoll, W. *Chem. Commun.* **2010**, *46*, 1908–1910. (b) Yameen, B.; Ali, M.; Neumann, R.; Ensinger, W.; Knoll, W.; Azzaroni, O. *Small* **2009**, *5*, 1287–1291. (c) Wang, L.; Sun, L.; Wang, C.; Chen, L.; Cao, L.; Hu, G.; Xue, J.; Wang, Y. *J. Phys. Chem. C* **2011**, *115*, 22736. (d) Ren, R.; Zhang, Y.; Nadappuram, B. P.; Akpınar, B.; Klenerman, D.; Ivanov, A. P.; Edler, J. B.; Korchev, Y. *Nat. Commun.* **2017**, *8*, 586. (e) Daiguji, H.; Yang, P.; Majumdar, A. *Nano Lett.* **2004**, *4*, 137–142. (f) Hou, X.; Liu, Y.; Dong, H.; Yang, F.; Li, L.; Jiang, L. *Adv. Mater.* **2010**, *22*, 2440–2443. (g) Zhang, H.; Hou, X.; Hou, J.; Zeng, J.; Tian, Y.; Li, L.; Jiang, L. *Adv. Funct. Mater.* **2015**, *25*, 1102–1110. (h) Zhang, H.; Tian, Y.; Hou, J.; Hou, X.; Hou, G.; Ou, R.; Wang, H.; Jiang, L. *ACS Nano* **2015**, *9*, 12264–12273. (i) Hou, X. *Adv. Mater.* **2016**, *28*, 7049–7064.
- (3) (a) Actis, P.; Rogers, A.; Nivala, J.; Vilozny, B.; Seger, R. A.; Jejelowo, O.; Pourmand, N. *Biosens. Bioelectron.* **2011**, *26*, 4503–4507. (b) Zhang, M.; Meng, Z.; Zhai, J.; Jiang, L. *Chem. Commun.* **2013**, *49*, 2284–2286. (c) Guo, W.; Xia, H.; Cao, L.; Xia, F.; Wang, S.; Zhang, G.; Song, Y.; Wang, Y.; Jiang, L.; Zhu, D. *Adv. Funct. Mater.* **2010**, *20*, 3561–3567. (d) Zhou, Y.; Guo, W.; Cheng, J.; Liu, Y.; Li, J.; Jiang, L. *Adv. Mater.* **2012**, *24*, 962–967. (e) Wen, L.; Liu, Q.; Ma, J.; Tian, Y.; Li, C.; Bo, Z.; Jiang, L. *Adv. Mater.* **2012**, *24*, 6193–6198.
- (4) (a) Kalman, E. B.; Vlasiouk, I.; Siwy, Z. S. *Adv. Mater.* **2008**, *20*, 293–297. (b) Actis, P.; McDonald, A.; Beeler, D.; Vilozny, B.; Millhauser, G.; Pourmand, N. *RSC Adv.* **2012**, *2*, 11638–11640. (c) Vilozny, B.; Actis, P.; Seger, R. A.; Vallmajo-Martin, Q.; Pourmand, N. *Anal. Chem.* **2011**, *83*, 6121–6126. (d) Vlasiouk, I.; Kozel, T. R.; Siwy, Z. S. *J. Am. Chem. Soc.* **2009**, *131*, 8211–8220. (e) Ali, M.; Ahmed, I.; Ramirez, P.; Nasir, S.; Cervera, J.; Niemeyer, C. M.; Ensinger, W. *Nanoscale* **2016**, *8*, 8583–8590. (f) Ramirez, P.; Cervera, J.; Ali, M.; Ensinger, W.; Mafe, S. *ChemElectroChem* **2014**, *1*, 698–705. (g) Gomez, V.; Ramirez, P.; Cervera, J.; Nasir, S.; Ali, M.; Ensinger, W.; Mafe, S. *Appl. Phys. Lett.* **2015**, *106*, 073701.
- (5) (a) Buchsbaum, S. F.; Nguyen, G.; Howorka, S.; Siwy, Z. S. *J. Am. Chem. Soc.* **2014**, *136*, 9902–9905. (b) Liu, M.; Zhang, H.; Li, K.; Heng, L.; Wang, S.; Tian, Y.; Jiang, L. *Adv. Funct. Mater.* **2015**, *25*, 421–426. (c) Miles, B. N.; Ivanov, A. P.; Wilson, K. A.; Doğan, F.; Japrun, D.; Edler, J. B. *Chem. Soc. Rev.* **2013**, *42*, 15–28. (d) Shi, W.; Friedman, A. K.; Baker, L. A. *Anal. Chem.* **2017**, *89*, 157–188. (e) Haywood, D. G.; Saha-Shah, A.; Baker, L. A.; Jacobson, S. C. *Anal. Chem.* **2015**, *87*, 172–187.
- (6) (a) *Nanofluidics*; Edler, J., Kim, M. J., Ivanov, A., Eds.; Royal Society of Chemistry: Cambridge, 2017. (b) Mawatari, K.; Tsukahara, T.; Tanaka, Y.; Kazoe, Y.; Dextras, P.; Kitamori, T. *Extended-Nanofluidic Systems for Chemistry and Biotechnology*; Imperial College Press: London, 2012.
- (7) (a) Dekker, C. *Nat. Nanotechnol.* **2007**, *2*, 209–215. (b) Schoch, R. B.; Han, J.; Renaud, P. *Rev. Mod. Phys.* **2008**, *80*, 839–883.
- (8) Sexton, L. T.; Horne, L. P.; Martin, C. R. *Mol. BioSyst.* **2007**, *3*, 667–685.
- (9) Siwy, Z. *Adv. Funct. Mater.* **2006**, *16*, 735–746.
- (10) Chun, H.; Chung, T. D. *Annu. Rev. Anal. Chem.* **2015**, *8*, 441–462.
- (11) Vlasiouk, I.; Park, C.; Vail, S. A.; Gust, D.; Smirnov, S. *Nano Lett.* **2006**, *6*, 1013–1017.
- (12) Karnik, R.; Duan, C.; Castelino, K.; Daiguji, H.; Majumdar, A. *Nano Lett.* **2007**, *7*, 547–551.
- (13) Zhang, C.; Mcadams, D. A., II; Grunlan, J. C. *Adv. Mater.* **2016**, *28*, 6292–6321.
- (14) Ripley, R. L.; Bhushan, B. *Philos. Trans. R. Soc., A* **2016**, *374*, 20160192.
- (15) Hou, X.; Jiang, L. *ACS Nano* **2009**, *3*, 3339–3342.
- (16) Pérez-Mitta, G.; Albesa, A. G.; Trautmann, C.; Toimil-Molares, M. E.; Azzaroni, O. *Chem. Sci.* **2017**, *8*, 890–913.
- (17) Coulter, W. H. U.S. Patent 2,656,508, 1953.
- (18) Siwy, Z. S.; Powell, M. R.; Kalman, E.; Astumian, R. D.; Eisenberg, R. S. *Nano Lett.* **2006**, *6*, 473–477.
- (19) Pérez-Mitta, G.; Albesa, A. G.; Toimil-Molares, M. E.; Trautmann, C.; Azzaroni, O. *ChemPhysChem* **2016**, *17*, 2718–2725.
- (20) (a) Hanggi, P.; Bartussek, R. *Lect. Notes Phys.* **1996**, *476*, 294–308. (b) Hanggi, P.; Marchesoni, F. *Rev. Mod. Phys.* **2009**, *81*, 387–442.
- (21) (a) Sexton, L. T.; Horne, L. P.; Martin, C. R. *Mol. BioSyst.* **2007**, *3*, 667–685. (b) Siwy, Z. *Adv. Funct. Mater.* **2006**, *16*, 735–746. (c) Wei, C.; Bard, A. J.; Feldberg, S. W. *Anal. Chem.* **1997**, *69*, 4627–4633. (d) Siwy, Z.; Fulinski, P. *Phys. Rev. Lett.* **2002**, *89*, 198103.
- (22) Howorka, S.; Siwy, Z. *Chem. Soc. Rev.* **2009**, *38*, 2360–2384.
- (23) Fleischmann, M.; Hendra, P. J.; McQuillan, A. J. *Chem. Phys. Lett.* **1974**, *26*, 163–166.
- (24) Chen, Y.; Wang, X.; Hong, M.; Erramilli, S.; Mohanty, P. *Sens. Actuators, B* **2008**, *133*, 593–598.
- (25) Ali, M.; Tahir, M. N.; Siwy, Z.; Neumann, R.; Tremel, W.; Ensinger, W. *Anal. Chem.* **2011**, *83*, 1673–1680.
- (26) Wang, X.; Chen, Y.; Gibney, K. A.; Erramilli, S.; Mohanty, P. *Appl. Phys. Lett.* **2008**, *92*, 013903.
- (27) Lin, L.; Yan, J.; Li, J. *Anal. Chem.* **2014**, *86*, 10546–10551.
- (28) (a) Fink, D.; Muñoz-Hernández, G.; Alfonta, L. *Sens. Actuators, B* **2011**, *156*, 467–470. (b) Fink, D.; Muñoz-Hernández, G.; Alfonta, L. *Nucl. Instrum. Methods Phys. Res., Sect. B* **2012**, *273*, 164–170. (c) Garcia-Arellano, H.; Muñoz H, G.; Fink, D.; Vacik, J.; Hnatowicz, V.; Alfonta, L.; Kiv, A. *Nucl. Instrum. Methods Phys. Res., Sect. B* **2018**, *420*, 69–75.
- (29) Hou, G.; Zhang, H.; Xie, G.; Xiao, K.; Wen, L.; Li, S.; Tian, Y.; Jiang, L. *J. Mater. Chem. A* **2014**, *2*, 19131–19135.
- (30) (a) Litvinchuk, S.; Tanaka, H.; Miyatake, T.; Pasini, D.; Tanaka, T.; Bollot, G.; Mareda, J.; Matile, S. *Nat. Mater.* **2007**, *6*, 576–580. (b) Hagihara, S.; Tanaka, H.; Matile, S. *J. Am. Chem. Soc.* **2008**, *130*, 5656–5657.
- (31) Pérez-Mitta, G.; Albesa, A. G.; Gilles, F. M.; Toimil-Molares, M. E.; Trautmann, C.; Azzaroni, O. *J. Phys. Chem. C* **2017**, *121*, 9070–9076.
- (32) Pérez-Mitta, G.; Marmisollé, W. A.; Albesa, A. G.; Toimil-Molares, M. E.; Trautmann, C.; Azzaroni, O. *Small* **2018**, *17*, 1702131.
- (33) Dixon, N. E.; Blakeley, R. L.; Zerner, B. *Can. J. Biochem.* **1980**, *58*, 481–488.
- (34) Cesareo, S. D.; Langton, S. R. *FEMS Microbiol. Lett.* **1992**, *99*, 15–21.
- (35) Heller, J.; Trescony, P. V. *J. Pharm. Sci.* **1979**, *68*, 919–921.
- (36) Piccinini, E.; Bliem, C.; Reiner-Rozmanc, C.; Battaglini, F.; Azzaroni, O.; Knoll, W. *Biosens. Bioelectron.* **2017**, *92*, 661–667.

- (37) Dutta, D.; Chandra, S.; Swain, A. K.; Bahadur, D. *Anal. Chem.* **2014**, *86*, 5914–5921.
- (38) Lian, H.-T.; Liu, B.; Chen, Y.-P.; Sun, X.-Y. *Anal. Biochem.* **2012**, *426*, 40–46.
- (39) Niu, X.; Li, X.; Pan, J.; He, Y.; Qiu, F.; Yan, Y. *RSC Adv.* **2016**, *6*, 84893–84905.
- (40) Huang, C.-P.; Li, Y.-K.; Chen, T.-M. *Biosens. Bioelectron.* **2007**, *22*, 1835–1838.